Short Communication

Fabrication and Characterization of Nanocrystalline Nickel with a Grain Size Gradient by Direct Current Electrodeposition

Haitao Ni[1,], Peng Li[1], Zhaodong Wang[1], Zexin Zou[1], Mincai Zhao[1], Lixia Wang[2] and Jiang Zhu[1,*]*

[1] College of Materials and Chemical Engineering, Chongqing University of Arts and Sciences, Yongchuan, Chongqing 402160, China
[2] College of Mechanical and Electrical Engineering, Chongqing University of Arts and Sciences, Yongchuan, Chongqing 402160, China
[*]E-mail: htniok@163.com (H.N.); Jiangzhu415@163.com (J.Z.)

Two series of nanocrystalline nickel samples with a grain size gradient and symmetric structure were successfully prepared by direct current electrodeposition under the guidance of deposition kinetics. The microstructures of as-deposited samples were characterized by X-ray diffraction, scanning electron microscopy, transmission electron microscopy and microhardness measurements. Comprehensive and quantitative analysis of the grain size indicated that the microstructure gradient was composed of nanograins varying from 20-100nm. Electronic microcosmic observation and microhardness analysis revealed that the samples with a grain size gradient had good structural homogeneity and symmetry.

1. INTRODUCTION

Due to the excellent performance of nanostructured materials, the preparation and processing of these materials is a hot research topic. For example, the limitations of homogeneous nanostructured metals have been gradually revealed by materials scientists. Recently some studies have shown that gradient nanostructures are an effective way to overcome the shortcomings of homogeneous nanostructures and develop their performance advantages [1-4]. Therefore, increasing attention is being focused on the preparation of nanostructures that include a gradient in the grain size, composition or orientation.

To date, nanostructured materials with a gradient in the grain size are usually prepared by imposing a gradient in the plastic deformation or in the physical or chemical deposition process. Based

on an understanding of the deformation-induced grain refinement process, it would be straightforward to produce gradient nanostructures on the material surface or throughout the entirety of thin materials as a result of gradients in the deformation amount and deformation rate. Attempts to prepare a gradient structure by imposing a gradient in the plastic deformation have been made. Nanostructured layers of copper, iron and some alloys with a gradient have been successfully obtained by a surface mechanical attrition treatment, a surface mechanical grinding treatment, and so on [5-7]. Nonetheless, in some cases, a gradient nanostructure cannot be controlled and adjusted well. In this regard, it seems that a gradient in the physical or chemical deposition process could produce some flexibility in the nanostructure. According to the correlation between the grain size and deposition conditions, a specific gradient change in grain size can be obtained by dynamic control of the deposition conditions. Previous research already confirmed that nickel with a grain size gradient from 10 nm to tens of microns can be prepared by electrochemical deposition by controlling the deposition rate and other conditions [8]. More specifically, a gradient in the thickness and grain size of the deposited samples can be obtained.

To intuitively understand the rolling deformation behaviour of metals with a grain size gradient, a symmetric nanocrystalline nickel sample with a gradient in the grain size distribution, which ranged from 20 nm to 100 nm, was designed. Although different methods have been applied for the fabrication of nanocrystalline nickel, electrodeposition is an effective and the preferred approach [9-17]. It is clear that a gradient during the chemical deposition process can effectively meet the requirements of grain-size gradient-structured sample preparation. A variety of characterization techniques were used to evaluate the overall quality of the gradient samples.

2. EXPERIMENTAL

In the present investigation, a direct current electrodeposition method was chosen to prepare gradient nanocrystalline nickel with a symmetrical structure. As shown in Figure 1, two series of samples with grain size gradients were designed.
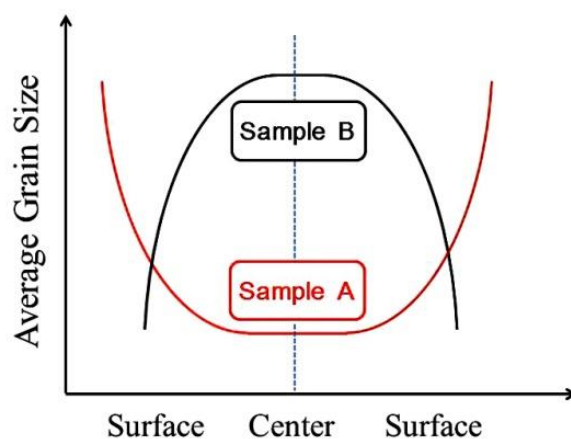
Figure 1. Grain size variation of two series of gradient nanocrystalline nickel with symmetrical structure

For convenience, one group was referred to as sample A, and the other group was referred to as sample B. For sample A, the average grain size was decreased from the surface region to the centre region of the sample, while the trend for sample B was reversed. Beyond that, it was necessary to ensure that the centre region had a sufficient thickness for the subsequent experimental study of rolling deformation. Based on a literature survey, a modified Watts-type nickel solution was selected for the electrolyte system. Each bath mainly included nickel sulfate hexahydrate (230 g/L), nickel chloride (45 g/L), boric acid (40 g/L), saccharin (2.50 g/L) and sodium dodecyl sulfate (0.05 g/L). For the electrodeposition process, a well-polished and activated high-purity copper plate was used as the cathode, and a high-purity electrolytic nickel plate was used as the anode. The temperature of the electrodeposition baths was maintained at 55℃. To achieve accurate control of the grain size distribution, a series of orthogonal experiments was used to quickly determine proper operating conditions. For a given electroplating bath composition, the results indicated that the top three factors that affected the grain size were the current density, pH value and stir speed. During the continuous electrodeposition process, the stir speed was controlled at 320 rpm, and the pH value was adjusted to 2.7 ±0.1 by adding sulfuric acid. The current densities and operation process curves are shown in Figure 2. A current density range of 1.7 A/dm^2~15.0 A/dm^2 was used. The whole electrodeposition process lasted for 3 hours.

Two series of samples with dimensions of 30 mm (length) × 20 mm (width) were obtained. After the samples were peeled from the cathode, the as-deposited samples were first trimmed into a rectangular sheet of 24 mm (length) × 12 mm (width) and then cut into small pieces for further inspection.
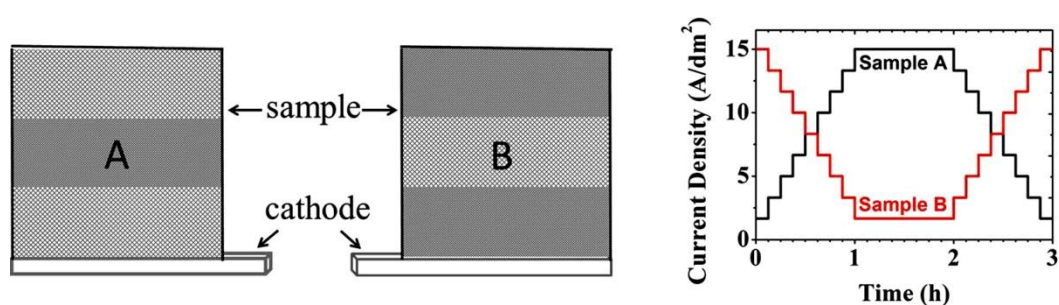
Figure 2. Electrodeposit current densities of two series of gradient nanocrystalline nickel samples with symmetrical structure

To evaluate the quality of the electrodeposited samples, microstructure analysis and microhardness measurements were conducted on the gradient samples at various depths along the thickness direction. In particular, more attention was paid to the layers corresponding to the deposition current densities of 1.7 A/dm^2, 8.3 A/dm^2, and 15.0 A/dm^2. The microstructures of two series of samples were mainly analyzed by X-ray diffraction (XRD), scanning electron microscopy (SEM) and transmission electron microscopy (TEM). XRD measurements were carried out on a Rigaku D/MAX 2500 PC diffractometer. The diffraction data were collected in a fixed time mode (0.02° per step) from

40° to 128° with a step time of 0.5 s. The SEM observations were performed with a Carl Zeiss Gemini SEM 300 operated at 3 kV. The TEM observations were performed with a FEI TECNAI 20 operated at 200 kV. The hardness measurement was conducted on an HVS-1000 microhardness tester using a load of 100 g and a dwell time of 10 seconds.

3. RESULTS AND DISCUSSION

To explore the uniformity and symmetry of the as-prepared gradient nanocrystalline nickel samples, the electrodeposition rate was varied and is summarized and displayed in Figure 3 for the given operating conditions. It can be clearly seen that the electrodeposition rate increases with increasing electrodeposition current density. Further regression analysis shows that the electrodeposition rate is linear with the electrodeposition current density when the electrodeposition current density does not exceed 5.0 A/dm^2. As the electrodeposition current density increases, the relationship between the electrodeposition rate and electrodeposition current density gradually deviates from the initial linearity. Similar results have been reported in the previous investigation [17-18]. According to the theory of electrochemistry, the electrodeposition rate v (mm/h) for nickel coating could be deduced as:

$$v = 1.23 \times 10^{-2} \cdot \eta \cdot i \tag{1}$$

Where η is the current efficiency, i is the cathode current density (A/dm^2). Following Eq.(1), electrodeposition rate is closely related to the current efficiency and current density. Therefore, it is easy to understand that the electrodeposition rate displays a general ascending trend with the increase of current density. Moreover, with the increasing current density, the current efficiency will tend to decline, and thus the electrodeposition rate shows a significant downward deviation.
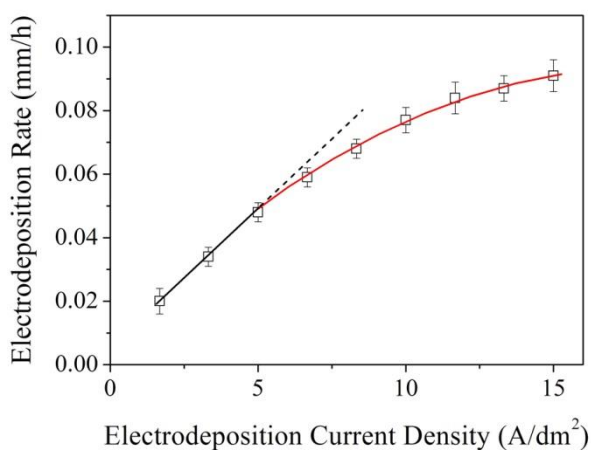
Figure 3. Electrodeposition rate of nanocrystalline nickel under different current densities

Based on the above data and the electrodeposition time, the theoretical value of the sample thickness is calculated. For gradient samples A and B, the theoretical thickness is determined to be ~

0.212 mm and ~ 0.162 mm, respectively. In the current experiment, the thickness measurement of the electrodeposited sheets for gradient samples A and B was found to be ~ 0.208 mm and ~ 0.164 mm, respectively. Thus, the relevant electrodeposition rate data are reliable. Moreover, this also indirectly indicates that the symmetric gradient samples are likely to be successfully prepared.

Figure 4 shows the XRD results of the as-prepared sample at various depths. All the XRD patterns can be identified as pure nickel with a face-centred cubic structure (JCPDS NO. 04-0850). Further analysis reveals that there is no significant difference in the angle of the diffraction peaks at different layers, indicating that the internal stress of each region is almost the same. For example, the (111) and (200) diffraction peaks for sample A broaden from the surface to centre, indicating that the average size of the grains located at the centre region is smaller than that of grains located in the surface region. Quantification of the XRD results shows that the average size of the grains located at the surface region is ~ 75 nm, while that of grains located at the centre region is ~ 20 nm. Furthermore, the correlation between the crystallographic texture and electrodeposition conditions is also explored. The texture coefficient is used to evaluate the preferential crystallite orientation of various electrodeposited layers. From the results listed in Table 1, an assessment of texture coefficient shows that the samples have an obvious (200) preferential orientation when compared to the data of standard non-textured samples. Some electrodeposited layers also display a (111) preferential orientation.
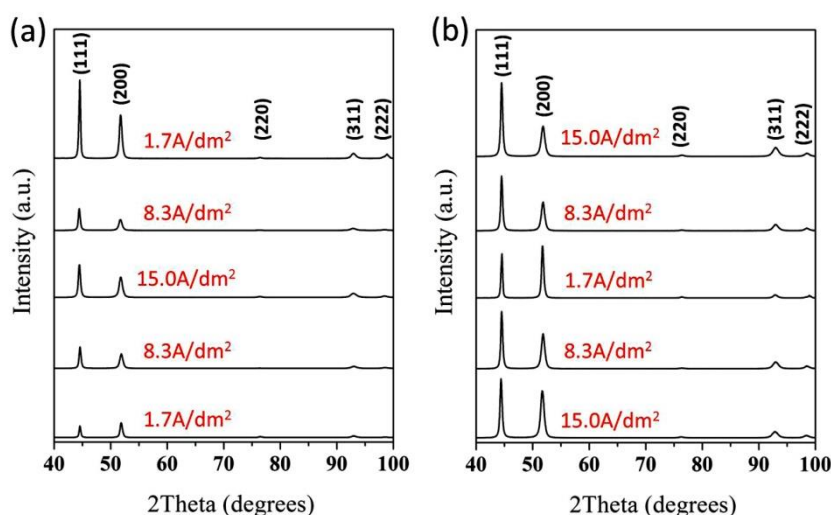
Figure 4. XRD results of as-deposited sample at various depths corresponding to different current densities.

Table 1. Texture coefficient for the two series of gradient nanograined nickel samples

Sample	Layer	Current Density (A/dm^2)	(111)	(200)	(220)	(311)	(222)
A	I	1.7	1.47	1.87	0.08	0.46	1.03
A	II	8.3	1.72	1.94	0.07	0.73	0.75
A	III	15.0	1.40	2.00	0.16	0.84	0.80

A	IV	8.3	1.54	2.38	0.05	0.66	0.68
A	V	1.7	1.01	3.04	0.34	0.67	0.46
B	I	15.0	1.59	1.48	0.13	0.91	0.92
B	II	8.3	1.47	1.73	0.08	0.80	0.94
B	III	1.7	1.01	2.83	0.11	0.34	0.85
B	IV	8.3	1.43	1.96	0.07	0.80	0.87
B	V	15.0	1.33	2.45	0.09	0.66	0.72

Figure 5 displays typical SEM images of the layers corresponding to the deposition current densities of 1.7 A/dm^2, 8.3 A/dm^2, and 15.0 A/dm^2. As shown in Figure 5(a), the grain size is distributed uniformly according to low-magnification microscopy. For each layer, observation at high-magnification indicates that the grains are equiaxed in shape, as shown in Figure 5(b)-(d). A horizontal comparison at the same magnification indicates that higher current density would be conducive to the refinement of the grain structure, which is consistent with a previous reported investigation on direct-current electrodeposited nanocrystalline nickel. Numerous experiments have reported that high current density can promote nucleation and inhibit grain growth [10, 19-26].
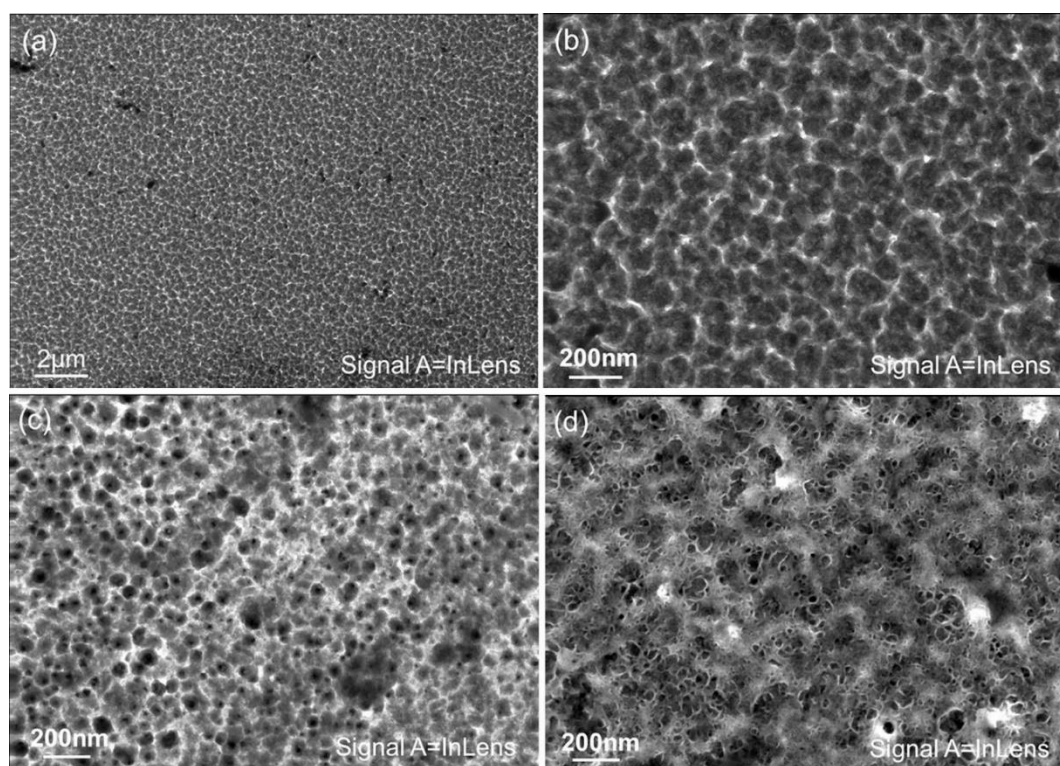
Figure 5. Typical SEM images of the layers corresponding to the different deposition current densities.(**a**) 1.7A/dm^2; (**b**) 1.7A/dm^2; (**c**) 8.3A/dm^2; (**d**) 15.0A/dm^2.

On the basis of the general theory of electrodeposition, the degree of cathodic polarization increases accordingly with the increase of current density, which makes the electrodeposition reaction proceed at a higher over-potential. Meanwhile, the increase of over-potential could accelerate nucleation, and the number of nuclei increases. Therefore, the larger the current density in the

electrodeposition process, the smaller the size of nanocrystals. However, it is also important to note that excessive current density will increase the driving force of grain growth, resulting in an increment of grain size. On the other hand, in the current study, the pH used is relatively low. While Ni^{2+} is reduced to Ni, a small amount of H^+ can also be electronically reduced to H_2 on the electrode. Under the effect of hydrogen evolution, hydrogen provides more nucleation centers for nanocrystals during the cathodic reduction of nickel ions. Statistical results show that the average grain sizes of three layers corresponding to the deposition current densities of 1.7 A/dm^2, 8.3 A/dm^2, and 15.0 A/dm^2 are 96±8 nm, 42±6 nm and 24±5 nm, respectively.

Figure 6 displays TEM results of the surface layer (1.7 A/dm^2) and centre layer (15.0 A/dm^2) of sample A. It is clearly seen that the grains located in the surface layer are indeed larger than those located in the centre layer. For each layer, more than 200 grains chosen from the TEM dark-field images were used to analyze the overall variation in the grain size distribution. The quantitative analysis indicates that a large proportion (more than 80%) of grains have a diameter greater than 70 nm in the centre layer, while a large proportion (more than 70%) of grains have a diameter less than 40 nm in the surface layer.
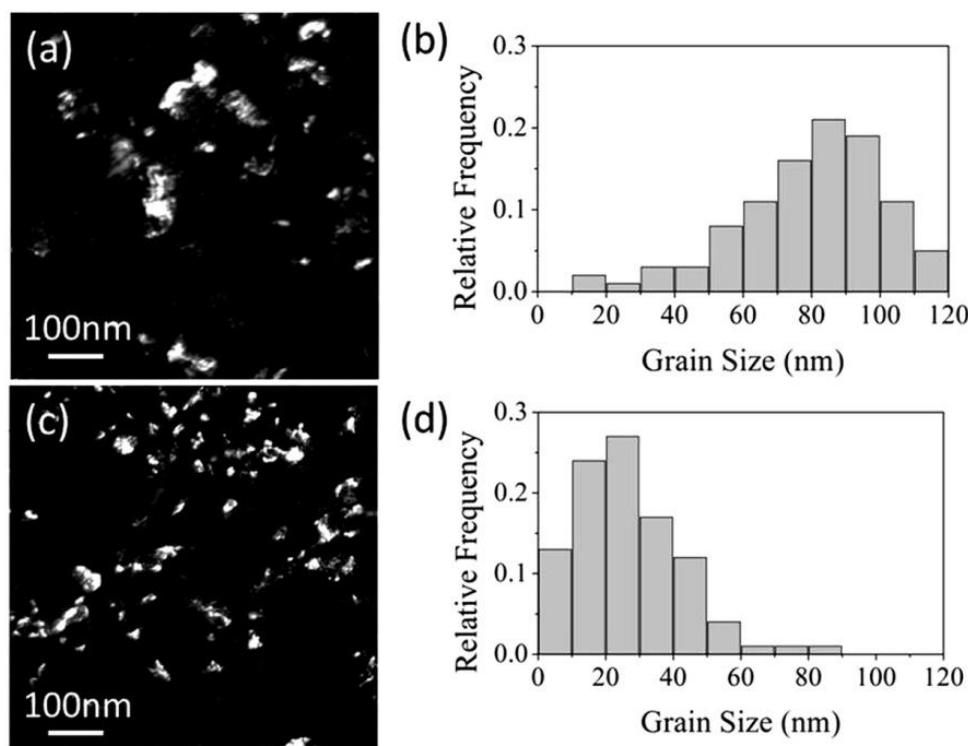
Figure 6. TEM results of surface layer (1.7A/dm^2) and center layer (15.0A/dm^2) of the sample A. (**a**) dark field images of surface layer; (**b**) grain size distribution in surface layer; (**c**) dark field images of center layer; (**d**) grain size distribution in center layer.

Measurement of the hardness measurement is another method commonly used to evaluate the quality of nanostructured metals in addition to average grain size and grain size distribution analysis. A good relationship between the grain size and hardness for electrodeposited nanocrystalline nickel has

been established. Therefore, to check the macroscopic homogeneity of the as-prepared gradient sample, the hardness is measured to rapidly obtain the grain size distribution on the macroscopic scale based on a grain size-hardness correlation. The hardness results of the samples at different layers are shown in Figure 7 and Table 2. For each layer, there is a small change in hardness at 9 positions, indicating that each layer consists of a homogeneous microstructure. With the central layer as the boundary, the hardness values of sample A and sample B at the same positions on both sides on the boundary are symmetric. Moreover, the hardness increases from the surface layer to the centre layer for sample A, while the hardness decreases from the surface layer to the centre layer for sample B. These hardness trends could be explained by the Hall-Petch relationship. The grain size of sample A decreases from the surface layer to the centre layer, while sample B is the opposite.
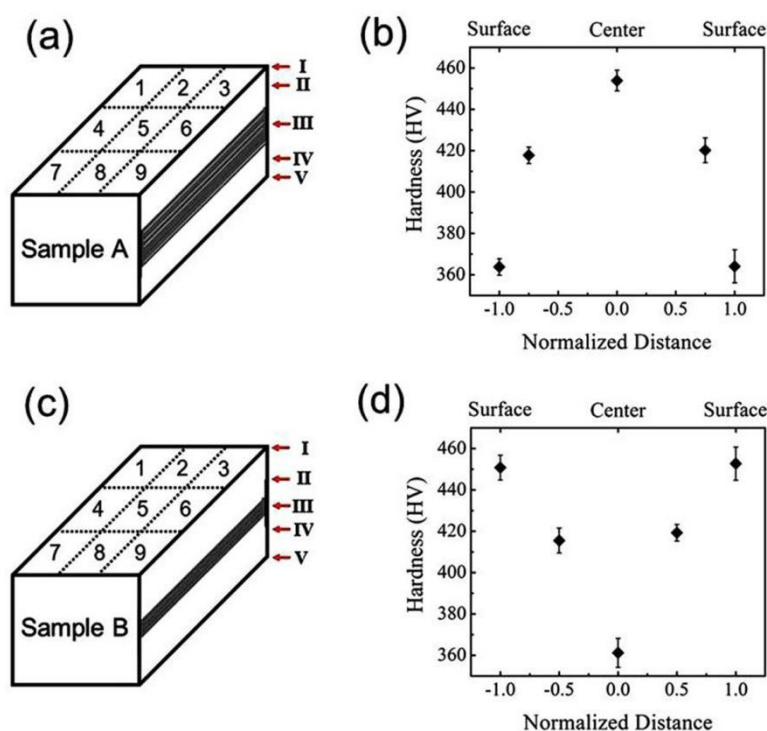
Figure 7. Hardness results of gradient nanocrystalline nickel at different layers.

Table 2. Vichers Microharness results of the two series of gradient nanograined nickel samples

Sample	Layer	Positions									Average
		1	2	3	4	5	6	7	8	9	
A	I	362.2	359.9	355.8	364.5	355.8	354.7	367.4	364.7	365.8	361.2
A	II	417.7	418.5	419.1	414.7	416	417.7	420.8	417.1	418.3	417.8
A	III	444.9	448.9	454.7	457.1	453.7	454.1	448.2	456.6	455.9	452.7
A	IV	418.6	414.5	420.4	421.1	424.2	420.1	418	423.6	421.7	420.2
A	V	367.6	362.1	363.8	361.2	369.2	366.2	359.9	362.1	362.3	363.8
B	I	447.4	449.7	456.6	447.2	456.5	448.5	448.5	446.7	455.7	450.8
B	II	418.0	415.0	412.1	415.0	412.1	415.6	410.2	421.0	420.8	415.5
B	III	364.9	373.3	361	360.1	365.7	367.7	366.7	361.3	356.6	364.1
B	IV	420	416.4	416.4	421	419	419.2	419.9	420.9	421.3	419.3
B	V	456.6	449.4	457.9	456.1	456.7	454.9	449.4	447.1	456.7	453.9

In particular, according to the Hall-Petch relationship, a linear regression equation is established for hardness (HV) and the inverse square root of the grain size ($d^{-1/2}$), as shown in Figure 8. In our present study, based on least squares fitting, the relationship between hardness and grain size can be expressed as follows:

$$HV = 2.7 + 8.1d^{-1/2}$$

(2)

The Hall-Petch slope is determined to be 8.1. Considering the measurement errors of the hardness and grain size, the calculated allowable variation of the Hall-Petch slope could range from 5.3 to 12.2, which agrees well with previous investigations on electrodeposited nanocrystalline nickel [27-28].
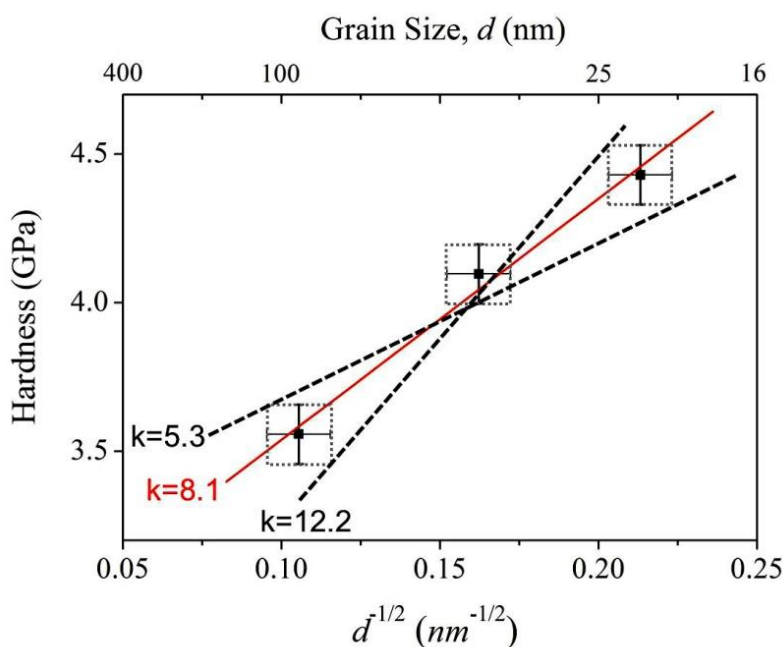
Figure 8. The relationship between hardness and grain size of the gradient nanocrystalline nickel samples

4. CONCLUSION

In summary, gradient nanocrystalline nickel samples with symmetric structures were successfully prepared by direct current electrodeposition. Microstructural characterization showed that the as-deposited samples comprised nanograins with sizes in the range of 20-100 nm and had a good structural homogeneity. The texture coefficient determined with the help of X-ray diffraction patterns revealed that the as-deposited samples had an obvious (200) preferred orientation. Electron microscopy observations, X-ray diffraction and microhardness analysis revealed that the samples exhibited grain size gradients from the surface to the centre. With the central layer as the boundary, the gradient samples had good symmetry. Further analysis of the Hall-Petch relationship between the hardness and grain size illustrated that the determined microstructural parameters and microhardness data were reasonable.

References

1. K. Lu, *Science*, 345 (2014) 1455.
2. M. Yang, Y. Pan, F. Yuan, Y. Zhu and X. Wu, *Mater. Res. Lett*., 4 (2016)1.
3. X.L. Wu, P. Jiang, L. Chen, J.F. Zhang, F.P. Yuan and Y.T. Zhu, *Mater. Res. Lett*., 2 (2014) 185.
4. Y.F. Wang, C.X. Huang, M.S. Wang, Y.S. Li and Y.T. Zhu, *Scripta Mater*., 150 (2018) 22.
5. B. Chen, G. Zhang, L. Zhang and T. Xu, *Int. J. Adv. Manuf. Tech*., 94 (2017) 1.
6. W. Chen, Z.S. You, N.R. Tao, Z.H. Jin and L. Lu, *Acta Mater*., 125 (2017) 255.
7. W.L. Li, N.R. Tao and K. Lu, *Scripta Mater*., 59 (2008) 546.
8. Y. Lin, J. Pan, H.F. Zhou, H.J. Gao and Y. Li, *Acta Mater*., 153 (2018) 279.
9. N. Dong, C. Zhang, J. Li and P. Han, *Rare Metal Mat. Eng*., 45 (2016) 885.
10. F. Yang, W. Tian, H. Nakano, H. Tsuji, S. Oue and H. Fukushima, *Mater. Trans*., 51 (2010) 948.
11. A.M. El-Sherik and U. Erb, *J. Mater. Sci*., 30 (1995) 5743.
12. X. Liu, L. Shen, M. Qiu, Z. Tian, Y. Wang and K. Zhao, *Surf. Coat. Tech*., 305 (2016) 231.
13. B. Lv, Z. Hu, X. Wang and B. Xu, *Surf. Coat. Tech*., 270 (2015) 123.
14. K.R Mamaghani. *Int. J. Electrochem. Sci*., 12 (2017) 5023.
15. E. Moti, M.H. Shariat and M.E. Bahrololoom, *Mater. Chem. Phys*., 111 (2008) 469.
16. L. Shen, W. Zhuo, M. Qiu, W. Jiang, K. Zhao and C. Wang, *Mater. Sci. Tech*., 34 (2017) 419.
17. I. Bakonyi, E. Tóth-Kádár, L. Pogány, Á. Cziráki, I. Gerőcs, K. Varga-Josepovits, B. Arnold and K. Wetzig, *Surf. Coat. Tech*., 78 (1996) 124.
18. J.X. Kang, W.Z. Zhao and G.F. Zhang, *Surf. Coat. Tech*., 203 (2009) 1815.
19. M. Bhardwaj, K. Balani, R. Balasubramaniam, S. Pandey and A. Agarwal, *Surf. Eng*., 27 (2011) 642.
20. N.P. Wasekar, P. Haridoss, S.K. Seshadri and G. Sundararajan, *Surf. Coat. Tech*., 291 (2016) 130.
21. A. M. Rashidi and A. Amadeh, *Surf. Coat. Tech.,* 202 (2008) 3772.
22. M. Hayati, A. M. Rashidi and A. Rezaei, *Solid State Sci.,* 13 (2011) 163.
23. P.Q. Dai, H. Yu, Q. Li, *Trans. Mater. Heat Treatment*, 25 (2004) 1283.
24. L. Wang, Y. Gao, T. Xu, Q. Xue, *Mater. Chem. Phys.*, 99 (2006) 96.
25. V.F.C. Lins, E. S. Cecconello and T. Matencio, *J. Mater. Eng. Perform.*, 17 (2008) 741.
26. Y. R. Uhm, K. Y. Park and S. J. Choi, *Res. Chem. Intermed.*, 41 (2015) 4141.
27. G.D. Hughes, S.D. Smith, C.S. Pande, H. R. Johnson and R.W. Armstrong, *Scripta Metal. Mater*., 20 (1986) 93.
28. T.G. Nieh and J.G. Wang*, Intermetallics*, 13 (2005) 377.